

Effect of annealing temperature on microstructure and high-temperature tensile behaviour of Ti-6242S alloy produced by Laser Powder Bed Fusion

Riccardo Casati, Gabriele Boari, Alessandro Rizzi & Maurizio Vedani

To cite this article: Riccardo Casati, Gabriele Boari, Alessandro Rizzi & Maurizio Vedani (2021) Effect of annealing temperature on microstructure and high-temperature tensile behaviour of Ti-6242S alloy produced by Laser Powder Bed Fusion, European Journal of Materials, 1:1, 72-83, DOI: [10.1080/26889277.2021.1997341](https://doi.org/10.1080/26889277.2021.1997341)

To link to this article: <https://doi.org/10.1080/26889277.2021.1997341>



© 2021 The Author(s). Published by Informa UK Limited, trading as Taylor & Francis Group.



Published online: 30 Nov 2021.



Submit your article to this journal [↗](#)



Article views: 769




View related articles [↗](#)



View Crossmark data [↗](#)

Effect of annealing temperature on microstructure and high-temperature tensile behaviour of Ti-6242S alloy produced by Laser Powder Bed Fusion

Riccardo Casati^a , Gabriele Boari^a, Alessandro Rizzi^b and Maurizio Vedani^a

^aDepartment of Mechanical Engineering, Politecnico di Milano, Milano, Italy; ^bBeam-IT, Fornovo di Taro, PR, Italy

ABSTRACT

This work is focussed at investigating the properties of additive manufactured Ti-6242S, a Ti alloy with excellent mechanical strength and stability up to 550°C. Special attention is given to the effect of different heat treatment routes on microstructure and high-temperature mechanical behaviour of the Ti-6242S alloy produced by Laser Powder Bed Fusion. Annealing was performed in the α/β field (at 940°C, 960°C, 980°C) or above the β transus (at 1050°C). Annealing step was followed by Ar gas cooling and ageing at 595°C. The as-built material exhibits high strength and anisotropic behaviour, showing lower fracture elongation in the direction parallel to the build platform. Heat treatments are responsible for a reduction of material strength but an increase in fracture elongation. Tensile tests at high temperature show that the best heat treatment for applications up to 300°C is the annealing at 940°C followed by Ar cooling and ageing. For applications at higher temperatures (namely 550°C, 750°C) the annealing step should be performed above the β transus temperature, at 1050°C, to achieve the best tensile properties.

ARTICLE HISTORY

Received 6 September 2021
Accepted 21 October 2021

KEYWORDS

Additive manufacturing;
Ti-6242S;
heat treatments;
tensile properties;
microstructure

Introduction

Titanium alloys are key lightweight materials for high-performance applications due to their unique combination of properties including high specific strength, fatigue resistance, fracture toughness, together with

CONTACT Riccardo Casati  riccardo.casati@polimi.it  Department of Mechanical Engineering, Politecnico di Milano, Milano 20133, Italy

© 2021 The Author(s). Published by Informa UK Limited, trading as Taylor & Francis Group.

This is an Open Access article distributed under the terms of the Creative Commons Attribution License (<http://creativecommons.org/licenses/by/4.0/>), which permits unrestricted use, distribution, and reproduction in any medium, provided the original work is properly cited.

good corrosion behaviour (ASM International Handbook, 1990). Aerospace is the largest market for titanium, with its reference industry consuming about 80% of its global production. Currently, Ti alloys account for 25–30% of the weight of modern aeronautical engines and can be used for components operating at temperatures up to 500–600 °C (Fujishiro, Froes, & Eylon, 1984). However, the use of such alloys is to some extent limited by their cost, which is higher than that of other competing materials. This is the result of the expensive extractive process of the metal from its ores, along with the costly operations related to fabrication of parts, including shaping and machining (Bodunrin, Chown, & Omotoyinbo, 2021). Additive manufacturing (AM) applied to Ti alloys is therefore of paramount interest because not only it enables the production of lightweight components featuring unprecedented complex shapes, but it can also lead to a reduction of total cost for production of parts (Wohlers Associates, 2020). So far, Ti6Al4V received most of the attention due to its high strength-to-weight ratio and wide processability, becoming the most widespread Ti alloy for AM parts (Liu & Shin, 2019; Wohlers Associates, 2020). Despite its excellent room-temperature properties, the Ti6Al4V alloy cannot be employed for parts operating above 300 °C, limiting the range of applications (Eylon, Fujishiro, Postans, & Froes, 1984). To overcome this limitation, this work is focussed at studying the properties of a Ti-6242S alloy manufactured by Laser Powder Bed Fusion (LPBF). Such alloy shows promising mechanical strength, microstructure stability and creep resistance up to 550 °C (Eylon et al., 1984). Being also a weldable near- α Ti alloy (Rajan, Wanjara, Gholipour, & Kabir, 2020), it is also expected to have good LPBF processability. The main alloy elements are Al and Mo, which stabilize the α - and β -phase, respectively. Sn and Zr are added as solid solution strengthener of the α -phase, while Si improves thermal stability and high-temperature mechanical behaviour (Chamanfar, Pasang, Ventura, & Misiolek, 2016; Imai, Yamane, Matsumoto, Vidal, & Velay, 2019). Ti-6242S is currently used for engine parts of motorsport vehicles and for aerospace components, e.g. discs and impellers of gas turbines (Max, Alexis, Larignon, & Perusin, 2020). The wrought Ti-6242S is typically used after a specific heat treatment able to promote a bimodal structure with globular α and transformed β grains. To achieve this microstructural configuration, the material is annealed below the β transus temperature, in the $\alpha + \beta$ field, after a hot working step. The ratio between globular α and transformed β grains affects creep properties and high-temperature yield strength of the material. Usually, the typical volume fraction of globular α is ~20% for a good combination of tensile and creep properties. The fully lamellar microstructure, which is obtained when the material is annealed above the β transus and air cooled, is preferred

when the creep characteristics are favoured over the tensile properties. Regardless of the heat treatment temperature (above or below the β transus), the material is finally aged to improve and stabilize the mechanical properties (Fujishiro et al., 1984; Hosseini, Morakabati, Abbasi, & Hajari, 2017; Lutjering, 1998).

To the best of authors' knowledge, two papers were published on similar alloys processed by LPBF in recent years, while the present research was still on-going. In 2020, Fan and Yang published a paper focussing on the Si-free version of the Ti-6242 alloy (Fan & Yang, 2020). They investigated the mechanical properties of the alloy in the as-built state and after direct ageing, which led to material failure before yielding. In 2021, Fleißner-Rieger and co-workers published a work on microstructure and mechanical behaviour of the Ti-6242S, the Si-bearing version of the Ti-6242. They performed tensile tests at room and high temperature on stress relieved specimens printed with longitudinal axis normal to the building platform (Fleißner-Rieger et al., 2021).

This work is aimed at investigating the effect of different heat treatment schedules on microstructure and high-temperature mechanical behaviour of Ti-6242S alloy produced by LPBF. Samples were printed along two orthogonal directions and heat treated either in the α/β field, at 940 °C, 960 °C, 980 °C, or above the β transus, at 1050 °C. After high-temperature annealing, all samples were eventually aged at 595 °C. The microstructure of the alloy in different conditions was characterized by optical microscope, field emission scanning electron microscope (FE-SEM) and electron back scattered diffraction (EBSD). Tensile tests were performed at room temperature (RT), 300 °C, 550 °C and 750 °C.

Materials and methods

Ti-6242S gas-atomized powder was supplied by General Electric AP&C featuring a particle size range between 20 and 63 μm . The composition of the powder measured by Inductively Coupled Plasma Atomic Emission Spectrometry (ICP) according to the ASTM-E2371 standard is shown in Table 1.

Samples for microstructure analysis and mechanical tests were produced by EOS M290 LPBF system with selecting a power of 310 W and a scan speed of 1250 mm/s. Layer thickness and hatch distance were set at 0.06 mm and 0.12 mm, respectively, and the building platform was

Table 1. Chemical composition (in weight %) of the investigated Ti-6242s powder.

Al	Sn	Zr	Mo	Si	Fe	O	C	N	H	Ti
6.19	1.95	3.93	1.96	0.08	0.12	0.12	0.01	0.01	0.002	bal.

pre-heated at 80 °C. Laser scanning direction was rotated 67° after each layer completion, so all direction parallel to the build platform (in the XY plane) are substantially identical. These parameters result from a process-optimization activity which is not discussed in this paper. Heat treatments were performed by two industrial vacuum furnaces, namely a TAV HTP 60/60/60 sn-720 and a TAV HTP 30/35/60 sn-628. Annealing temperatures ranged between 940 °C and 1050 °C, whereas holding time was kept constant at 1 hour. Ar gas was used for cooling with rate of about 80 °C/min. Ageing treatment was performed at 595 °C for 8 hours. Finally, the printed parts were separated from the build platform by wire cutting after the heat treatment stage.

Samples for microstructure analysis were mounted and ground down to 2500 grit sandpaper for 90 s with a contact force of 30 N, using water as lubricant. Specimens were then polished by diamond pastes with decreasing grain size, down to 1 µm, and by colloidal suspension of silica. Five 50× images of vertical and horizontal polished sections of samples were taken by a Nikon Eclipse LV150NL optical microscope and used for density measurements by ImageJ software. Kroll (100 mL H₂O, 2 mL HF, 5 mL HNO₃) was used as etchant solution. The Nikon Eclipse LV150NL was also used along with Zeiss SMT EVO 50 FE-SEM to investigate microstructural features of the as-built (AB) and heat-treated alloys.

Differential scanning calorimetry (DSC) analysis was performed by Setaram Labsys system under Ar atmosphere in the temperature range between 20 °C and 1500 °C with a heating rate of 10 °C/min.

Tensile tests were performed at RT, 300 °C, 550 °C and 750 °C. Tests at RT were performed with a ProLine testing system setting according to the ASTM E8/E8M-21 standard. High temperature tensile tests were performed by a Instron universal testing machine according to the ASTM E21-17e1. Tensile tests specimens with gauge length of 28 mm and diameter of 6 mm were machined out from round bar with length of 88 mm and diameter of 11 mm. The tensile tests were replicated three times for each condition.

Results and discussion

Microstructure analysis of the as-built alloy

The Ti-6242S alloy revealed to be processable by LPBF. Indeed, no cracks were present on both vertical and horizontal sections of samples and almost full density was achieved (relative density = 99.99%). Typical optical micrographs of etched sections taken parallel to the building direction ([Figure 1a](#)) show the presence of bands, as also noted in

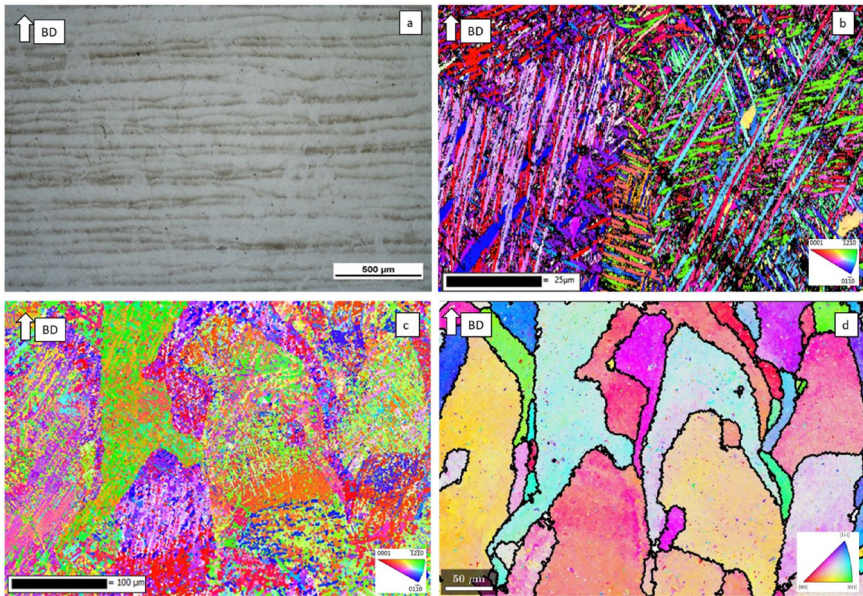


Figure 1. (a) Optical micrograph of the AB Ti-6242S alloy, (b,c) orientation maps relative to the Z axis (i.e. building direction) of the vertical section (i.e. parallel to the building direction) at 2500 \times and 1000 \times , (d) reconstructed orientation map of prior β grains from orientation map shown in (c).

(Fleißner-Rieger et al., 2021; Thijs, Verhaeghe, Craeghs, Van Humbeeck, & Kruth, 2010) for Ti-6242S and Ti6Al4V alloys produced by LPBF. Banding is likely due to different content of alloying elements within each melt pool, resulting in an inhomogeneous reaction to the etchant (Fleißner-Rieger et al., 2021; Thijs et al., 2010). The fully α' martensitic microstructure of the AB material is shown though the orientation maps relative to the building axis in Figure 1b and c. The crystallographic orientations of α' are limited by the local transformation from prior body centred cubic (bcc) β phase to hexagonal close packed (hcp) α' phase governed by the Burgers orientation relationship (Burgers OR): $\{1\ 1\ 0\}_{\beta} // \{0\ 0\ 1\}_{\alpha'}$; $\langle 1\ 1\ 1 \rangle_{\beta} // \langle 1\ -2\ 0 \rangle_{\alpha'}$ (Burgers, 1934). Prior β grain structure was reconstructed according to Burgers OR through the MTEX Matlab script (<https://mtextoolbox.github.io/index.html>) and it is shown in Figure 1d. Coarse β grains grew epitaxially along the building direction through several deposited layers. Indeed, it is worth noting that while the layer thickness was 60 μm , some grains shown in Figure 1d are in the order of a few hundreds of micrometres. The rapid cooling to the process temperature (build platform temperature = 80 $^{\circ}\text{C}$) led to the transformation of the parent β grains into a martensitic structure.

Calorimetric analysis

DSC analyses were performed to estimate the β transus temperature, which is needed to properly design the heat treatments. The thermogram of the AB Ti-6242S alloy is shown in Figure 2. The β transus peak is found at about 1020 °C, which is in good agreement with that measured in (Fleißner-Rieger et al., 2021) for the same alloy (1017 ± 3 °C). The endothermic peak at 938 °C roughly corresponds to the half of phase transformation at which α and β phases are present in the same concentration. The exothermic peak at ~660 °C is probably due to the precipitation of intermetallic particles, that was shown to occur in a similar temperature range (Carson, 2016; Fan & Yang, 2020), however we have no evidence for this.

Microstructure analysis of heat-treated alloys

DSC results were used to select four different annealing temperatures, namely: 940 °C, 960 °C, 980 °C and 1050 °C. The first three temperatures were chosen below the β transus to obtain bimodal microstructures with different ratios of α grains and transformed β grains, whereas 1050 °C was chosen to achieve a fully transformed β microstructure. After annealing the alloys were aged at 595 °C, as recommended in (Carson, 2016). Representative optical and FE-SEM micrographs of heat-treated samples are shown in Figures 3 and 4. The microstructure of specimens heated above the β transus temperature (Figures 3a and 4a) is characterized by

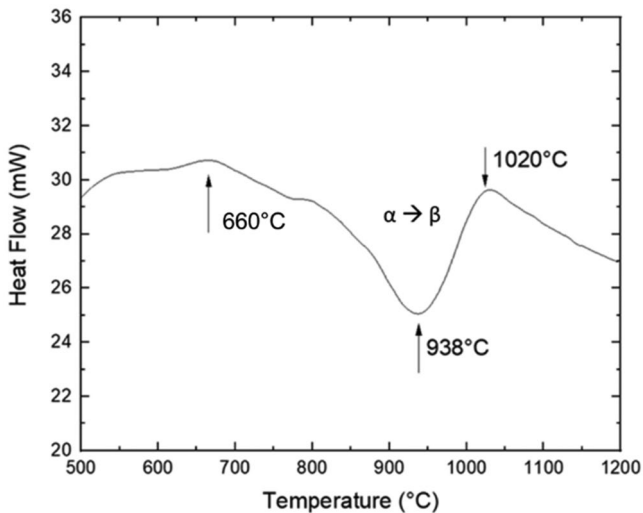


Figure 2. DSC curve of the AB Ti-6242s alloy.

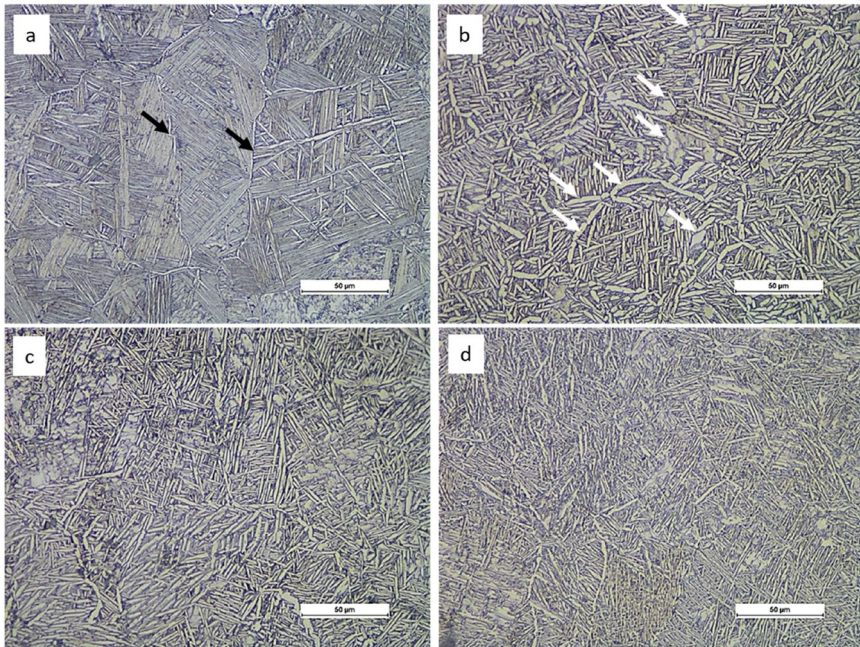


Figure 3. Optical micrographs of the alloy investigated annealed at: (a) 1050 °C, (b) 980 °C, (c) 960 °C, (d) 940 °C and cooled in Ar gas. The black arrows in (a) and the white arrows in (b) highlight layers of α phase at prior β grain boundaries and α globules/plates, respectively.

transformed β grains showing alternated α/β lamellae. An α layer forms at prior β grains boundaries, as pointed out by black arrows in the micrograph of Figure 3a. The microstructure of specimens annealed at 980 °C, shown in Figures 3b and 4b, is composed mainly by β transformed regions and by α plates and globules, both pointed out by arrows in Figure 3b. Samples treated at 960 °C and 940 °C show similar but finer microstructural features (Figure 3c and d). The microstructures depicted in the present study of LPBF processed alloys treated in the α/β range are different from the bimodal (duplex) structure that is usually obtained by annealing a wrought Ti-6242S in the same temperature range, as reported for instance in (Fujishiro et al., 1984; Lutjering, 1998). The latter is promoted by recrystallization processes, and it is characterized by coarser globular α grains in a matrix of transformed β grains (Fujishiro et al., 1984; Lutjering, 1998).

Ti₃Al precipitates are expected to form during ageing treatment (Carson, 2016; Fujishiro et al., 1984), but they were not observed by FE-SEM presumably due to their small size. However, as it can be seen from the FE-SEM images of Figure 4c and d, ageing has also an effect

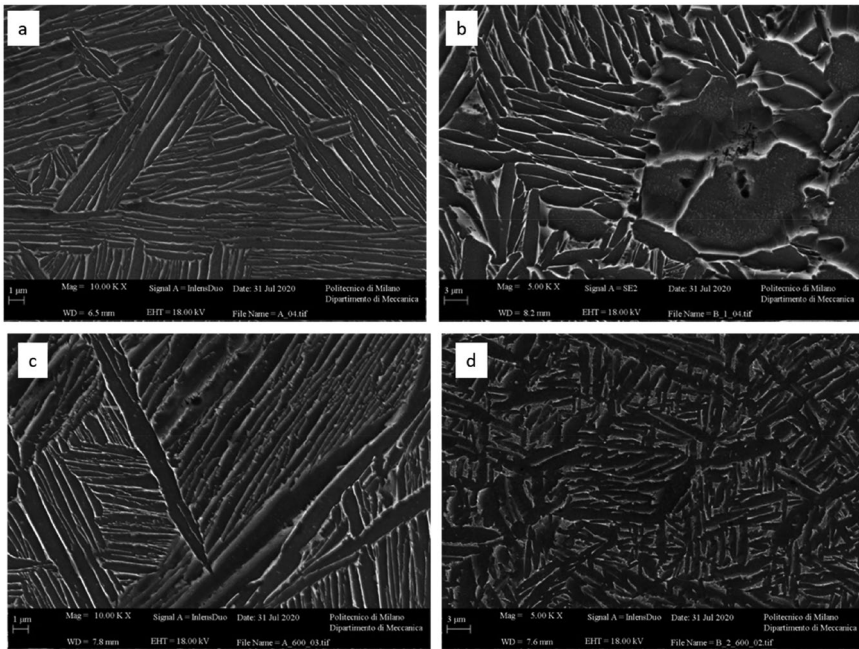


Figure 4. FE-SEM images of samples annealed at (a) 1050 °C, (b) 980 °C, (c) 1050 °C+595 °C and (d) 980 °C+595 °C. After high temperature annealing at 980 °C or 1050 °C, all samples were cooled down to RT with Ar gas and in (c) and (d) aged at 595 °C.

on the microstructure of annealed samples leading to the fragmentation of the lamellae, especially for the sample annealed at 980 °C.

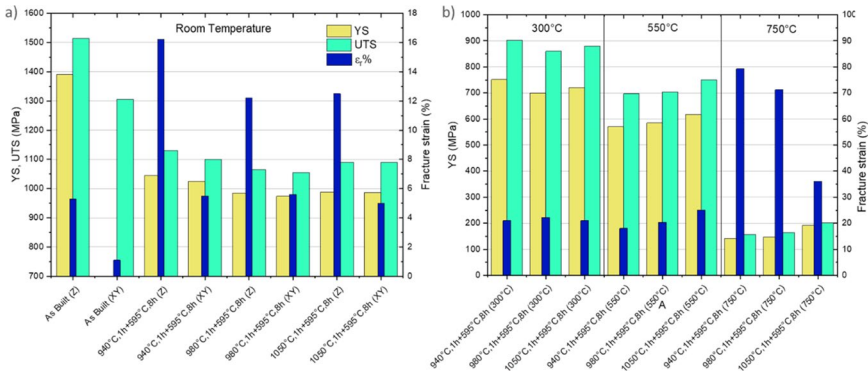
Tensile properties

The tensile properties of AB and heat-treated specimens with longitudinal axis parallel and normal to the building direction, i.e. in the Z direction and in the XY plane, are collected in Table 2 and plotted in the histogram of Figure 5a. The AB material has an anisotropic behaviour, showing high strength and low ductility, especially when the load is applied parallel to the XY plane. Some AB samples printed with longitudinal axis in the XY plane failed before yielding. The low ductility of the AB alloy is due to the fully martensitic microstructure, whereas the anisotropic behaviour is likely related to the coarse columnar grains that grow epitaxially along the building direction and have their longitudinal axis normal to the loading direction.

The heat treatment is responsible for the reduction in yield strength (YS) and ultimate tensile strength (UTS), but a clear increase in fracture

Table 2. Tensile properties of as-built and heat-treated Ti-6242s alloy tested at RT, 300, 550 and 750 °C.

Specimen condition	Printing orientation	Testing temperature [°C]			
		YS [MPa]	UTS [MPa]	ϵ_r [%]	
As-Built	Z	22	1390 ± 14	1515 ± 7	5.3 ± 0.5
As-Built	XY	22	n.a.	1305 ± 50	1.1 ± 0.1
940 °C, 1h + 595 °C, 8h	Z	22	1045 ± 4	1130 ± 0	16.2 ± 0.3
940 °C, 1h + 595 °C, 8h	XY	22	1025 ± 4	1101 ± 0	5.5 ± 2.1
980 °C, 1h + 595 °C, 8h	Z	22	985 ± 5	1064 ± 4	12.2 ± 0.3
980 °C, 1h + 595 °C, 8h	XY	22	974 ± 3	1055 ± 4	5.6 ± 0.5
1050 °C, 1h + 595 °C, 8h	Z	22	988 ± 4	1090 ± 0	12.5 ± 2.1
1050 °C, 1h + 595 °C, 8h	XY	22	986 ± 2	1091 ± 1	5.0 ± 1.5
940 °C, 1h + 595 °C, 8h	Z	300	751 ± 1	902 ± 2	21.0 ± 0.5
980 °C, 1h + 595 °C, 8h	Z	300	700 ± 6	860 ± 3	22.2 ± 1.0
1050 °C, 1h + 595 °C, 8h	Z	300	720 ± 7	880 ± 3	21.0 ± 3.5
940 °C, 1h + 595 °C, 8h	Z	550	572 ± 9	697 ± 8	18.0 ± 1.0
980 °C, 1h + 595 °C, 8h	Z	550	585 ± 0	703 ± 7	30.3 ± 2.1
1050 °C, 1h + 595 °C, 8h	Z	550	617 ± 1	750 ± 8	25.0 ± 0.7
940 °C, 1h + 595 °C, 8h	Z	750	141 ± 16	156 ± 12	79.2 ± 4.9
980 °C, 1h + 595 °C, 8h	Z	750	147 ± 2	163 ± 2	71.2 ± 3.8
1050 °C, 1h + 595 °C, 8h	Z	750	192 ± 0	202 ± 2	36.1 ± 3.8

**Figure 5.** Tensile properties of the Ti-6242s heat treated according to different routes at (a) room temperature, measured along the Z direction and in the XY plane, and at (b) 300, 550 and 750 °C, measured along the Z direction.

elongation (ϵ_r) of the material. Tensile properties at RT of the heat-treated alloy are affected by the α/β ratio and α colony size in β transformed grains. Typically, higher α/β ratio results in higher YS and UTS and lower ϵ_r owing to the different intrinsic properties of HCP and BCC phases (Hosseini et al., 2017). The interfaces between lamellae within each colony are not effective barriers to slip and dislocations can expand rapidly (Lutjering, 1998), whereas the interface between colonies is more effective against slip and, as a result, colony size is an important parameter to determine mechanical properties. The colony size depends on temperature and time of annealing (Lutjering, 1998). The colony size of

samples treated at 1050 °C are in the range 50–100 μm , whereas that of samples treated below β transus are smaller (about 30–50 μm). The specimens annealed at 940 °C have the highest percentage of α because they are treated just above the endothermic peak at 938 °C, that corresponds to the half of phase transformation to β , moreover they have smaller microstructural features (α globules, plates, colonies), therefore the UTS and YS of specimens annealed at 940 °C are higher than those of the other samples. Although the heat treatment reduced the alloy strength, it is beneficial for the alloy ductility. The increase in ductility after heat treatments is mainly attributed to the decomposition of α' martensite into an α/β microstructure. It is worth mentioning that the alloy preserves an anisotropic behaviour, mainly in terms of fracture elongation, also after the annealing steps.

The tensile properties of the heat-treated Z specimens tested at 300, 550 and 750 °C are collected in Table 2 and Figure 5b. The specimens annealed at 940 °C and aged maintain the highest tensile strength up to 300 °C. The fracture elongation at 300 °C of all specimens is about 20%, regardless of annealing temperature. The highest strength values at 550 °C and 750 °C are attained by the specimens annealed at 1050 °C. The worse tensile properties of specimens annealed in the $\alpha + \beta$ field at the highest temperatures can be attributed to the element partitioning during annealing, leading to a lower concentration of α stabilizer elements in β region (Fleißner-Rieger et al., 2021; Hosseini et al., 2017). A significative partitioning effect is responsible for the reduction of Al (α stabilizer) in prior β grains and consequently, the precipitation of the strengthening particles is less effective in such regions (Hosseini et al., 2017). The precipitation of abundant and well dispersed Ti_3Al particles throughout the microstructure is of paramount importance to achieve high mechanical properties at high temperature (Carson, 2016; Fujishiro et al., 1984).

For sake of comparison, it is worth mentioning that YS and UTS of forged Ti-6242S alloy at 480 °C (UTS = 735 MPa, YS = 564 MPa) (<https://www.timet.com/assets/local/documents/datasheets/alphaalloys/6242.pdf>) are lower than tensile strength values achieved in this work at 550 °C. This

Summary and conclusions

Crack-free almost fully-dense Ti-6242S samples were produced by LPBF and used to investigate on the effect of different heat treatment schedules on microstructure and high temperature mechanical behaviour the alloy. Ti-6242S alloy samples were heat treated either in the α/β field or above the β transus at 1050 °C, and consecutively aged at 595 °C. The heat

treatments substantially changed the martensitic microstructure typical of the as built material. In particular, the microstructure of the specimens treated above the β transus was characterized by transformed β grains made up by alternated α and β lamellae and surrounded by an α layer at boundaries. The microstructure of specimens annealed below the β transus was composed mainly by α plates and globules and β transformed grains. All heat treatment routes were responsible for the reduction of material strength, but an increase in ductility. Tensile tests at high temperature show that the most performing heat treatment for applications up to 300 °C is the annealing at 940 °C followed by Ar cooling and ageing. For applications up to 750 °C the annealing step should be better performed above the β transus temperature, at 1050 °C. Even though a more in-depth analysis, including creep, fatigue and fracture toughness tests, is needed to thoughtfully assess the mechanical behaviour of the material, the outcome of this work suggests that LPBF can be considered as a promising method to produce Ti-6242S structural parts for high temperature applications.

Acknowledgments

The Italian Ministry of Education, University and Research is acknowledged for the support provided through the Project “Department of Excellence LIS4.0 – Lightweight and Smart Structures for Industry 4.0”. The authors acknowledge Ing. Rasheed Michael Ishola for his support with Matlab software and SEM analysis.

Disclosure statement

No potential competing interest was reported by the authors.

ORCID

Riccardo Casati  <https://orcid.org/0000-0002-2796-8439>

References

- ASM International Handbook Committee. (1990). *ASM metals handbook volume 2 – Properties and selection nonferrous alloys and special-purpose materials*. ASM International.
- Bodunrin, M. O., Chown, L. H., & Omotoyinbo, J. A. (2021). Development of low-cost titanium alloys: A chronicle of challenges and opportunities. *Materials Today: Proceedings*, 38, 564–569.

- Burgers, W. G. (1934). On the process of transition of the cubic-body-centered modification into the hexagonal-close-packed modification of zirconium. *Physica*, 1(7-12), 561–586.
- Carson, C. (2016). Heat treating of titanium and titanium alloys. In *Heat treating of nonferrous alloys* (Vol. 4E, 670 p.). ASM international.
- Chamanfar, A., Pasang, T., Ventura, A., & Misiolek, W. Z. (2016). Mechanical properties and microstructure of laser welded Ti-6Al-2Sn-4Zr-2Mo (Ti6242) titanium alloy. *Materials Science and Engineering: A*, 663, 213–224.
- Eylon, D., Fujishiro, S., Postans, P. J., & Froes, F. H. (1984). High-temperature titanium alloys – A review. *JOM Journal of the Minerals Metals and Materials Society*, 36(11), 55–62.
- Fan, H., & Yang, S. (2020). Effects of direct aging on near-alpha Ti-6Al-2Sn-4Zr-2Mo (Ti-6242) titanium alloy fabricated by selective laser melting (SLM). *Materials Science and Engineering: A*, 788, 139533.
- Fleißner-Rieger, C., Pfeifer, T., Jörg, T., Kremmer, T., Brabetz, M., Clemens, H., & Mayer, S. (2021). Selective laser melting of a near- α Ti6242S alloy for high-performance automotive parts. *Advanced Engineering Materials*, 2001194. <https://doi.org/10.1002/adem.202001194>
- Fujishiro, S., Froes, F., & Eylon, H. D. (1984). Titanium alloys for high temperature applications – A review. *High Temperature Materials and Processes*, 6(1-2), 81–91.
- Hosseini, R., Morakabati, M., Abbasi, S. M., & Hajari, A. (2017). Development of a trimodal microstructure with superior combined strength, ductility and creep-rupture properties in a near alpha titanium alloy. *Materials Science and Engineering: A*, 696, 155–165.
- MTEX Toolbox website. <https://mtex-toolbox.github.io/index.html>
- Timetal 6-2-4-2 datasheet. <https://www.timet.com/assets/local/documents/data-sheets/alphaalloys/6242.pdf>
- Imai, H., Yamane, G., Matsumoto, H., Vidal, V., & Velay, V. (2019). Superplasticity of metastable ultrafine-grained Ti6242S alloy: Mechanical flow behavior and microstructural evolution. *Materials Science and Engineering: A*, 754, 569–580.
- Liu, S., & Shin, Y. C. (2019). Additive manufacturing of Ti6Al4V alloy: A review. *Materials & Design*, 164, 107552.
- Lutjering, G. (1998). Influence of processing on microstructure and mechanical properties of (α + β) titanium alloys. *Materials Science and Engineering Materials Science and Engineering A*, 243, 32–45.
- Max, B., Alexis, J., Larignon, C., & Perusin, S. (2020). Titanium alloy Ti-6242 for high temperature structural application. Static and dynamic mechanical properties and impact of ageing. *MATEC Web of Conferences*, 321, 11089.
- Rajan, S., Wanjara, P., Gholipour, J., & Kabir, A. S. (2020). Tensile properties, and fatigue behavior of linear friction-welded Ti-6Al-2Sn-4Zr-2Mo-0.1Si. *Materials*, 14(1), 30.
- Thijs, L., Verhaeghe, F., Craeghs, T., Van Humbeeck, J., & Kruth, J.-P. (2010). A study of the microstructural evolution during selective laser melting of Ti-6Al-4V. *Acta Materialia*, 58(9), 3303–3312.
- Wohlers Associates. (2020). Wohlers report 2020: 3D printing and additive manufacturing state of the industry. Wohlers Associates Inc, Fort Collins, Colorado.